Numerical and experimental state of identification battery pack lithium-ion

Dewi Anggraeni[1], Budi Sudiarto[3], Eriko Nasemudin Nasser[1], Wahyudi Hasbi[1], Yus Natali[2], Purnomo Sidi Priambodo[3]

[1]Research Center for Satellite Technology, National Research and Innovation Agency, Bogor, Indonesia
[2]Department of Electrical Engineering, Faculty of Engineering, Telkom University, Bandung, Indonesia
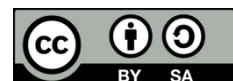[3]Department of Electrical Engineering, Faculty of Engineering, University of Indonesia, Depok, Indonesia

Article Info

ABSTRACT

Two key indicators of a battery management system (BMS) are the state of charge (SoC) and the state of health (SoH). Accurately estimating SoC is important to prevent potential issues. Additionally, space, computing time, and cost are important factors in hardware development. To address these considerations, the first-order extended Kalman filter (EKF) and adaptive extended Kalman filter (AEKF) models were selected due to their simpler data pre-processing and better accuracy. The study recommends using the first-order equivalent circuit model (ECM) method in conjunction with the EKF and AEKF algorithms due to their straightforward setup and efficient computational process. Analysis of the charge-discharge cycles shows that the AEKF method consistently outperformed the EKF method regarding SoC accuracy. Moreover, when given different initial SoC values, the AEKF method displayed superior SoC estimation accuracy compared to the EKF method. Moreover, while the accuracy of the EKF is diminished, the error value remains below 2.5% for up to 500 cycles. Additionally, the shorter computing time of the EKF method is a consideration for practical real-world implementation. Furthermore, experiments conducted over 500 cycles revealed that SoH estimation declined from 99.97% to 76.1947%, suggesting that the battery has reached the end of life (EOL) stage.

This is an open access article under the CC BY-SA license.

Corresponding Author:

Yus Natali
Department of Electrical Engineering, Faculty of Electrical Engineering, Telkom University
Daan Mogot Street, Kedaung Kali Angke, Cengkareng, West Jakarta 11710, Indonesia
Email: yusnatali@telkomuniversity.ac.id

1. INTRODUCTION

Lithium-ion batteries are extensively utilized for energy storage across a range of applications [1]. It has been favored in recent times due to its elevated energy levels, increased power density, and commendable longevity [2], [3], and utilized in electric vehicles, intelligent power grids, electronic apparatus, and powering synthetic aperture radar systems [4], aviation, and satellites [5]. In order to guarantee the well-being of the user, devices and the vehicle, it is imperative to operate within the confines of safety. As a result, the BMS, responsible for monitoring the rechargeable batteries, plays a critical role in safeguarding the electric vehicle and its instruments [6].

The two main functions in BMS are state of charge (SoC) and state of health (SoH). SoC is a crucial parameter that delineates the magnitude of electric charge accumulated within a battery in comparison to its complete capacity [7]. There is a great need for a dependable and precise method for estimating the SoC in battery management systems [8]. The SOC of a battery cannot be directly inferred; thus, it is often indirectly

approximated using data such as battery voltage, current, and temperature [9]. Several methods have been employed to assess the SoC in lithium-ion batteries [10]. To achieve a harmonious equilibrium between computational expenditure and the accuracy of estimations, the majority of the current approaches have implemented an equivalent-circuit model (ECM) to replicate the behaviors of batteries under both current and future load circumstances to estimate SoC [11]. The ECM possesses the potential to be construed as a model of limited complexity, which serves to closely approximate the dynamic characteristics of the battery voltage. This approximation is achieved through the utilization of linear state dynamics and a static nonlinearity that manifests itself in the model's output. Batteries have non-linear characteristics, and the estimation of SoC typically necessitates the employment of nonlinear extensions of the Kalman filter, such as the EKF, which is both highly recognized and widely employed [12]. However, the algorithm based on the EKF relies heavily on the accuracy of the battery model as well as the predetermined variables about the system noise, including mean value, pertinence, and covariance matrix. If the predetermined variables of the system noise are not properly configured, significant errors and divergence may occur. In the case of the SoC estimation, if inappropriate values for the noise covariance are utilized, the error would be substantial or even lead to divergence. Consequently, the utilization of AEKF has been employed to carry out real-time SoC estimation [13]. Moreover, even when precise model parameters are acquired, the connection between the open circuit voltage (OCV) and SoC will persistently alter due to battery aging. This occurrence impairs the durability of SoC estimation. Consequently, attaining high-precision SOC estimation in batteries subjected to prolonged usage proves challenging [14].

SoH is the condition where the battery can provide energy. This is used to determine the health condition of the battery after several charging-discharging cycles. This can also be said to be the lifespan of a battery pack [15]. The estimation of the SoH of the battery can be known either in real-time or not [16]. Estimation is divided into experimental and model-based techniques. Experimental estimation can accurately estimate SoH, and estimation can be achieved using several measurement activities on the battery to get the true value [17]. In this case, we estimate the SoH value when 1 cycle has been completed.

The relationship between SoC estimation accuracy and the model is very close, where a more complicated model will provide higher accuracy [18]. However, implementation on hardware is a concern in the study we conducted. In the study [19], the AEKF model has high accuracy. However, first-order AEKF is easier because it does not require data pre-processing, making it easier to implement in the microcontroller.

In addition to being easy to implement, it is necessary to take into account certain limitations concerning the available space and the system expenses when designing and implementing the hardware [20]. Space, computing time, and cost are important concerns in implementing BMS [20], [21]. Space is necessary for dense systems, particularly those related to aerospace systems [20]. Selecting a model that can be implemented on a single piece of hardware while ensuring reliable measurements and maintaining errors within a 2.5% margin [22]. is a key consideration for BMS development. This balance of efficiency and accuracy is an essential focus of our research, as it ensures the feasibility and reliability of the system's development.

The implementation performed in [23] based on electrochemistry, was conducted, where the data and calculations are controlled using FPGA hardware to make estimates. Moreover, stimulation devices were added to regenerate electrochemical impedance spectroscopy (EIS). This will result in additional device space. Furthermore, the calculating time will still be developed in their study. Similar to the study conducted in [24], A DC-servo loop regenerates frequency was added to the system estimation, resulting in additional devices which increase costs and extra space for integrated devices in estimating the SoC. An implementation based on data science, such as the study conducted in [25], uses an STM32 microprocessor, which has an affordable price. Nevertheless, there is an additional device in the form of Tensor Flow Lite Microcontrollers (TFLM) to execute model calculations based on data science. Moreover, the integrated hardware in the implementation based on the Kalman filter only requires one embedded device. The study in [26], uses a DEKF model embedded in an FPGA, and the implementation is carried out in [27], also uses an FPGA to calculate SoC estimation with the 2RC EKF model. Furthermore, in terms of both lower cost and how quickly calculations are performed in [28], The Raspberry Pi is used to calculate the EKF and UKF models. They specifically stated that the EKF model uses less power and shorter calculation times, even though the errors that appear are greater than the UKF. From the explanation above, it can be seen that the author's reasons for conducting a comparative study with the first-order EKF and AEKF were space efficiency, ease of integration in one device, less computing time, and lower prices.

To address the aforementioned problems, this study conducts the following investigations:
- Training two Kalman Filter models, namely the first-order EKF and AEKF, for SoC estimation.
- Examining the correlation between the M value, initial error, number of cycles, and computation time, and their impact on SoC estimation accuracy while maintaining standard accuracy.
- Analysing the changes in SoC estimation accuracy as the number of cycles increases.
- Assessing the health of a battery pack after completing 500 cycles.

2.   THE PROPOSED METHOD

In this study, the author's battery pack modeling method follows the study in [22], where a first-order ECM was used with parameters based on the author's previous research in the study [4]. The determination of the lithium-ion battery's state-of-charge is typically achieved through the utilization of the current integral, as depicted in (1). This assessment typically commences from an initial state-of-charge denoted as SoC_0 [29].

$$SoC_t = SoC_0 - \frac{\eta}{Q_{present}} \int_0^t I \qquad (1)$$

where SoC_t represents the real-time value of the state-of-charge at time t, SoC_0 denotes the initial value of the state-of-charge. Furthermore, η refers to the charge-discharge efficiency of a lithium-ion battery; here, we assume equal to one. $Q_{present}$ represents the effective capacity of the lithium-ion battery, and I denotes the measured current of the lithium-ion battery.

2.1. SoC algorithm-based EKF

Due to its inability to handle the nonlinear attributes of the battery model, the EKF has gained significant popularity in nonlinear applications. The fundamental concept behind the EKF involves employing a first-order Taylor expansion of the state and measurement functions to achieve local linearization. In the case of a nonlinear system, the following state-space equations in (2) can be employed to depict it [30]:

$$\begin{cases} X_k = f(X_{k-1}, u_k) = AX_{k-1} + Bu_{k-1} + w_{k-1} \\ \quad Y_k = g(X_k, u_k) = CX_k + Du_k + v_{k-1} \end{cases} \qquad (2)$$

where, X_k represents the state variable of the system. Y_k denotes the observation variable of the system. u_k signifies the input variable of the system. f denotes the state nonlinear function. g represents the measurement nonlinear function. w_{k-1} and v_k are Gaussian white noise with a mean of zero and covariance Q and R respectively.

The EKF algorithm proceeds through a series of iterations in accordance with the subsequent steps, first, initialize the mean $(\overline{X_0})$ and the covariance (P_0) of the initial system state X_0. Where E(.) is the expectation of the mean value.

$$\begin{cases} \qquad \bar{X}_0 = E(X_0) \\ P_0 = E[(X_0 - \bar{X}_0)(X_0 - \bar{X}_0)^T] \end{cases} \qquad (3)$$

The next step is Time update for the state and covariance prediction. The state and covariance prediction refers to (4).

$$\begin{cases} X_k^+ = f(X_{k-1}, u_{k-1}) + w_k \\ \quad P_k^- = C_k P_{k-1} C_k^T + Q_k \end{cases} \qquad (4)$$

The measurement process is updated with the Kalman Filter and update the covariance for (5) and (6).

$$K_k = P_k^- C^T (C P_k^- + R_k)^{-1} \qquad (5)$$

$$P_k = (I - K_k C_k) P_k (I - K_k C_k)^T + K_k R_k K_k^T \qquad (6)$$

2.2. SoC algorithm-based AEKF

Meanwhile, for the AEKF algorithm from (4) to (6) has the same equation as the EKF algorithm, whereas in the AEKF algorithm, the difference lies in the update status in (11), the next step is by adaptation of variable Q in (13), H in (14) and R in (15).

$$K_k^+ = \hat{X}_k + K_k e_k \qquad (11)$$

$$e_k = Y_k - g(\hat{X}_k, u_k) \qquad (12)$$

$$Q_k = K_k H_k K_k^T \qquad (13)$$

$$H_k = \frac{1}{M} \sum_{i=k-M+1}^k e_k e_k^T \qquad (14)$$

$$R_k = H_k - CP_kC^T \qquad (15)$$

The matrix C represents the Jacobian of the function g that is used to measure the data. The symbol "e_k" represents the disparity between the voltage measured at the terminal and the voltage that was previously estimated at the terminal. The definition of M has been explained in our study in [19]. Here, experiments are conducted to investigate the correlation between the variable M and the computational duration required for the estimation of SoC. Further examination will be explained in section 3.2.

2.3. SoH estimation

SoH is typically defined as the ratio of the nominal rated capacity at the time of manufacturing to the remaining maximum capacity at a given time. Therefore, the SoH could be formulated using (16) [31].

$$SoH(\%) = \frac{C_{present}}{C_{initial}} \, x \, 100\% \qquad (16)$$

where $C_{present}$ is the current battery's maximum capacity (Ampere hours) and $C_{initial}$ is the battery's initial maximum capacity. $C_{present}$ could be calculated with the total discharge current (I_{dchg}) capacity is obtained from the current capacity divided by the running time during the discharge process. Which is defined as (17).

$$C_{present}(t) = \int_0^t I_{dchg}(t)dt \qquad (17)$$

3.   METHOD

This section explains the research methods used in this study, including SOC estimation and its relationship to initial SOC disturbance. Additionally, it discusses the impact of SOC estimation on variable M, and also computation time for training the data, and lastly give an explanation for SoH estimation.

3.1. SoC estimation

The experiments were conducted over a span of six consecutive months, employing the subsequent elements: (a) 42 Ah of Lithium-ion battery pack; (b) a battery analyzer known as BST8-10A30 V; and (c) an electrical connection to the hub of the battery. The investigations were performed using charge- discharge cycles at a rate of 0.2 C at a temperature of 25 °C, interspersed with a relaxation interval of 30 minutes, thereby facilitating the attainment of relaxation concentration and the reestablishment of solid lithium particles to the point of equilibrium. Physical representation for the experiment platform on the Figure 1.

Figure 1. Physical representation of the experimental platform for testing Lithium-ion batteries

Data on the measurement of lithium battery packs is collected for a total of 500 cycles. These measurements include the terminal voltage U_T, Current I, capacity Q and time t. The current and voltage data are recorded at intervals of 20 seconds. The estimation of the SoC itself remains unaffected by the overall duration, as it is adjusted by a factor of 20 in the projected output calculation time. An illustration of the flow chart for estimating the SoC to train the two algorithms can be seen in Figure 2.

The test result data from BST8 will be organized to suit the requirements of the simulation. The necessary data includes cycle, current, voltage, and time data. For the simulation process, data from the 1st, 100th, 200th, 300th, 400th, and 500th cycles will be used to train two different models: first-order EKF and first-order AEKF. The parameter data will be directly obtained in the calculation process model. This will result in obtaining two sets of SoC estimation output data.

The real implementation of BMS cannot be separated from the ease of carrying out training data through models with light computing but is accurate. Therefore, the calculation time is a concern for this study. In this study, the Tic Toc function which is established in MATLAB software is used for the results of computing time calculations.
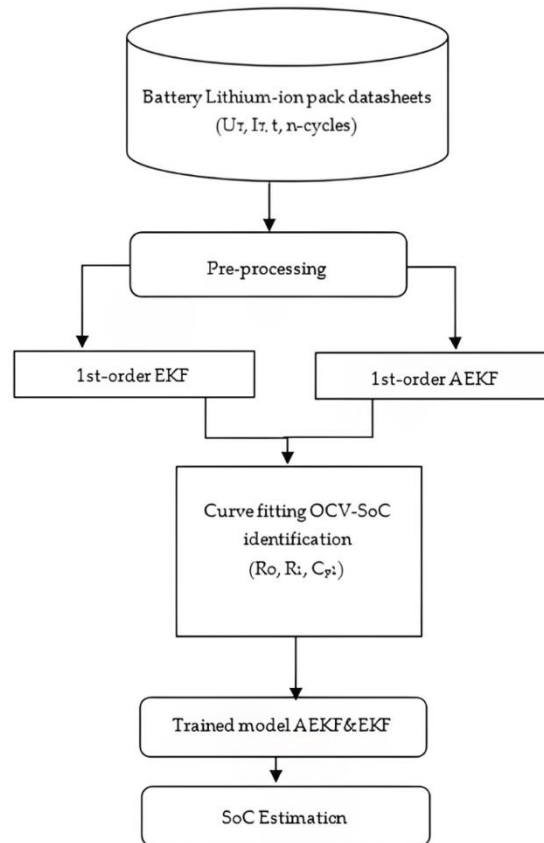

Figure 2. Flow diagram of the SoC estimation

3.2. The correlation between variable M and the duration of computational processes

Experiments were performed to examine the relationship between variable M in AEKF model and the computational time needed for estimating SoC (see Table 1). It can be observed that as the value of M decreases, there is an increase in the time required for calculations. We calculated the RSME value at M=1.2, because it has the smallest computation time, which shows a 5 x 10^{-1} value. Where the error value is still well controlled.

During the first cycle, we computed the processing time for both models. Based on the training data for SOC estimation, the calculation results are presented in Table 2. From these results indicate that the EKF model has a shorter computation time.

<div style="display:flex">

Table 1. M and the duration of computational processes

M	Time (s)	M	Time (s)
0.1	32.403	1	14.249
0.5	16.185	1.2	13.931

Table 2. Computational time

Model	Time (s)
EKF	7.117
AEKF	13.931

</div>

3.3. SoH estimation

To estimate the SoH, we calculate the stored capacity data based on the measurement results using equation (16). This calculation is performed at specific cycle intervals, namely at cycles 1, 100, 200, 300, 400, and 500, to observe the degradation trend over time. The estimation process focuses on the charge capacity Q_{cycle} that has completed a full cycle of charging and discharging, ensuring that the data reflects the actual usable capacity of the battery. By analyzing the capacity at these intervals, we are able to monitor changes in SoH and evaluate the battery's long-term performance.

4. RESULT AND DISCUSSION

This section explains the results of this study. including SOC estimation and its relationship to initial SOC disturbance. Additionally, it examines the impact of SOC estimation on variable M and computation time-training data, as well as the SoH estimation results.

4.1. SoC estimation result

The outcomes of SoC estimation for lithium-ion battery packs are presented, which were obtained using trained first-order models, EKF and AEKF. Furthermore, the impact of the accuracy of these estimation models on the integration of charging-discharging cycles is demonstrated in Figure 3. The black dash-dot line is the real SoC, while the blue cross line is the estimation result with EKF training, and the red triangle line is the estimated SoC from AEKF training. The simulation results across all cycles indicate that the EKF are more inconsistent (moves irregularly), which occurs in all cycles, namely in Figures 3(a)-3(f). Even though the EKF tends to move irregularly, the estimated line is close to the real SOC line. Meanwhile, AEKF shows a more consistent line. The estimated stability is 30% to 80%. This can be seen very much in the estimation with AEKF, as in Figure Figures 3(c) and 3 (e). Where the estimated starting point N=1 is very far from the real value, but slowly follows the real SoC line. Likewise, at the end, the estimate for the AEKF method moves below 30%. Although the SoC estimation with the AEKF method deviates at N=1 and at 30% of the SoC line, the RSME value shows that AEKF provides better accuracy than EKF, as shown in Tables 3 and 4 in the first cycle. The RSME in the EKF method in the first cycle shows 0.66%, which is much greater than the AEKF method with 0.35%. As the cycle progresses using the EKF technique, there is a corresponding increase in the magnitude of the error. This phenomenon becomes evident in cycle 1, as indicated by the RSME of 0.66%, which further escalates to 0.77% in cycle 500 (see Figure 3(f)). Similarly, the AEKF approach also exhibits a comparable pattern, with the RSME recorded at 0.35% in cycle 1 (see Figure 3(a)) and gradually averaging at 0.67%. Nevertheless, it is important to note that the EKF method demonstrates a more substantial upward trend in error, whereas the AEKF method experiences a relatively negligible increment in error.

4.2. Analysis of robustness using various initial SoC values

To determine the reliability of the method used, one way is to provide a different initial SoC value to determine the accuracy of the SoC estimate. Reliability will also be tested with increasing cycles. In this reliability test, we set the initial SoC value at 0.9, 0.8, and 0.7 for cycles 1, 100, 200, 300, 400, and 500. The training data of the EKF and AEKF methods can be seen in Table 3 and Table 4.

Table 3. RSME data of SoC estimation based on EKF methods

Cycle/Initial SoC	1	0.9	0.8	0.7
1	0.66	0.72	0.84	1.04
100	0.7	0.81	1.06	1.38
200	0.76	0.88	1.12	1.45
300	0.76	0.88	1.12	1.44
400	0.79	0.89	1.14	1.46
500	0.77	0.89	1.14	1.47

Table 4. RSME data of SoC estimation based on AEKF methods

Cycle/Initial SoC	1	0.9	0.8	0.7
1	0.35	0.29	0.44	0.67
100	0.41	0.39	0.68	1.05
200	0.41	0.39	0.69	1.06
300	0.41	0.39	0.69	1.06
400	0.41	0.39	0.7	1.08
500	0.41	0.41	0.71	1.1

The estimation of SoC is conducted using the EKF method. At the initial SoC of 0.9, the RSME indicates a value of 0.72%, which exhibits a gradual increase over successive cycles. The highest RSME is observed at 500 cycles, amounting to 0.89%. Similarly, for an initial SoC of 0.8, the highest RSME is recorded at cycles 400 and 500, reaching 1.14%. However, in the first cycle, it stands at 0.84%. Conversely, when the initial SoC is 0.7, the RSME is 1.04% in cycle 1, gradually escalating to 1.47% at cycle 500. Robustness tests conducted with varied initial SoCs illustrate that error values are higher for smaller initial SoCs, particularly at 0.7.

In the AEKF method, employing an initial SoC of 0.9, the RSME starts at 0.29% and slowly increases to 0.41% after 500 cycles. For an initial SoC of 0.8, the RSME is 0.44% in the first cycle, which further rises to 0.71% at cycle 500. Similarly, when the initial SoC is set at 0.7, the RSME begins at 0.67% and progressively climbs to 1.1% after 500 cycles. The reliability examination of the EKF and AEKF methods, conducted with different initial SoCs and increasing cycles, is summarized in the graphical representation provided in Figure 4 and Figure 5. It is evident from Figure 4 and Figure 5 that the AEKF method yields higher accuracy in SoC estimation compared to the EKF method.

In Figure 6, the progress of SoC estimation is presented, with disturbances occurring at k=1 with values of 0.7, 0.8, and 0.9 in the first cycle. The reliability of the EKF and AEKF models will be evaluated based on these disturbances. The cyan line represents the result of a disturbance process with an initial value of 0.7, labelled

as EKF7. Similarly, EKF8 indicates the SoC estimation line calculated using the EKF model with an initial disturbance value of 0.8, and so on, until the line marked AEKF9, which represents the initial disturbance at 0.9.

We can observe from Figure 6 that the estimation line tries to approach the real line, so this shows that after being disturbed in the form of the first initial value, the estimation line approaches the real line to get a good estimated value. Moreover, the AEKF estimate line shows an estimate line that is closer to the real line than the estimate line shown by estimates using the EKF model.
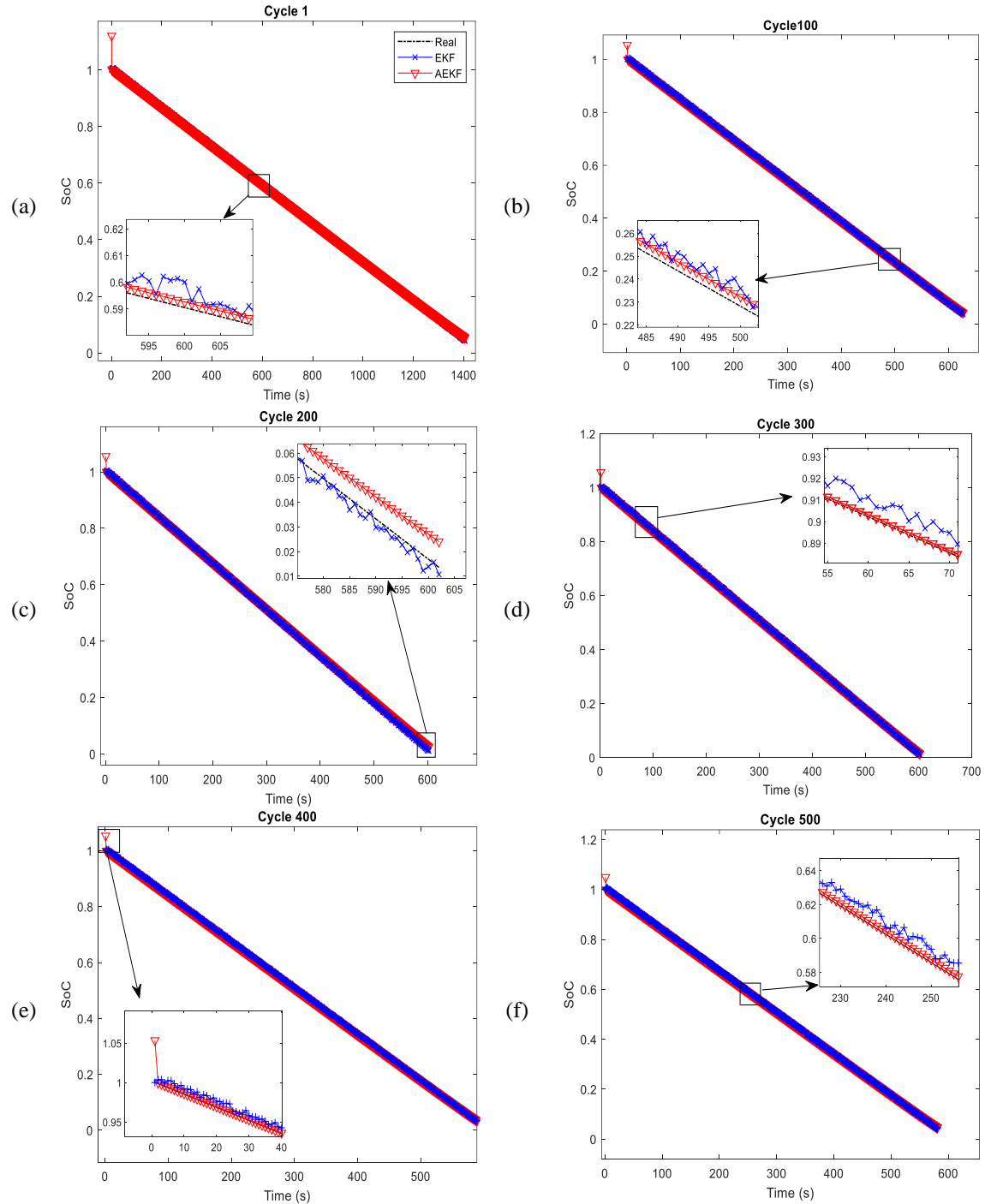
Figure 3. The EKF and AEKF performance results for (a) 1 cycle, (b) 100 cycles, (c) 200 cycles, (d) 300 cycles, (e) 400 cycles, and (f) 500 cycles
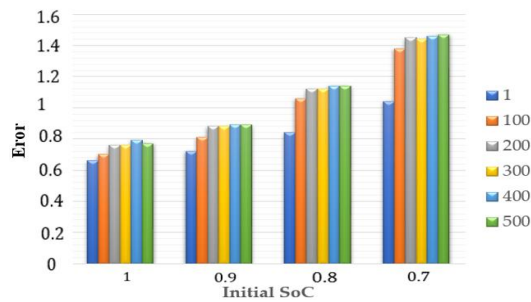
Figure 4. RSME result-based EKF methods in different initial SoC
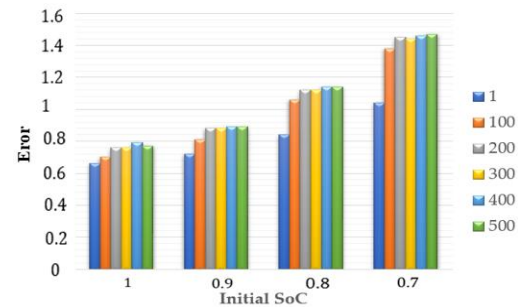
Figure 5. RSME result based AEKF method in different initial SoC
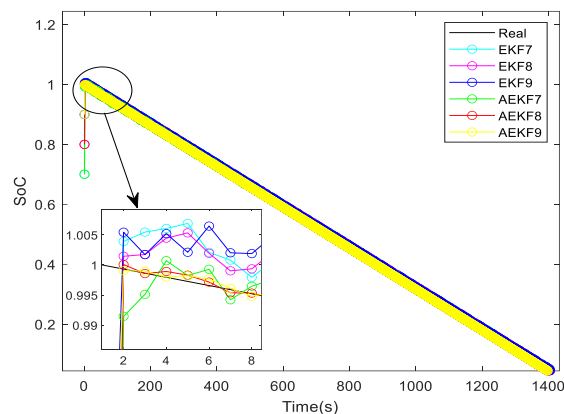
Figure 6. Analysis SoC estimation using various initial value

4.3. SoH estimation result

As explained in chapter 3.3. SoH estimation, the estimated SoH in each cycle can be seen in Table 5. Where the SoH percentage in the first cycle is still at 99.97% and is decreasing to 76.1947%. According to [32], [33], if the SoH percentage has already reached a range of 70-80%, the battery is on the EOL stage. This battery pack is a sensitive system; therefore, its EOL is aligned with that of electric vehicles to ensure safety and reliability.

Table 5. SoH estimation results

Cycle	SOH (%)	Cycle	SOH (%)
1	99.97	300	79.3571
100	83.3333	400	78.5714
200	79.762	500	76.1947

5. CONCLUSION

In this paper, we discuss the estimation of SoC using two different Kalman Filter techniques: the EKF and the AEKF. Both techniques use a first-order ECM for Lithium-ion battery packs. After analyzing the training data, we have made several significant conclusions. Firstly, we observed that the accuracy of the EKF method tends to decrease as the number of charge-discharge cycles increases. Secondly, a similar trend is noticed in the AEKF method, displaying behavior comparable to the EKF method. However, it's important to note that the AEKF method yields a smaller RMSE value compared to the EKF method. Moreover, while the accuracy of the EKF is diminished, the error value remains controlled below 2.5% for up to 500 cycles.

Thirdly, SoC estimation obtained using the AEKF method demonstrates superior accuracy when compared to the EKF method, particularly in robustness tests with different initial SoC. It is also observed that the EKF method requires less computational time than the AEKF method, which should be taken into consideration during the actual implementation stage. Lastly, we observed that the lithium-ion battery pack reaches EOL at 500 cycles.

AUTHOR CONTRIBUTIONS STATEMENT

This journal uses the Contributor Roles Taxonomy (CRediT) to recognize individual author contributions, reduce authorship disputes, and facilitate collaboration.

Name of Author	C	M	So	Va	Fo	I	R	D	O	E	Vi	Su	P	Fu
Dewi Anggraeni	✓	✓	✓	✓	✓	✓	✓	✓	✓	✓	✓		✓	✓
Budi Sudiarto		✓		✓	✓	✓	✓	✓	✓	✓	✓	✓		
Eriko Nasemudin Nasser	✓		✓		✓					✓		✓	✓	✓
Wahyudi Hasbi	✓				✓					✓		✓		✓
Yus Natali					✓					✓		✓		✓
Purnomo Sidi Priambodo		✓		✓	✓	✓	✓	✓		✓	✓	✓		

C : **C**onceptualization	I : **I**nvestigation	Vi : **Vi**sualization
M : **M**ethodology	R : **R**esources	Su : **Su**pervision
So : **So**ftware	D : **D**ata Curation	P : **P**roject administration
Va : **Va**lidation	O : Writing - **O**riginal Draft	Fu : **Fu**nding acquisition
Fo : **Fo**rmal analysis	E : Writing - Review & **E**diting	

CONFLICT OF INTEREST STATEMENT

The authors declare that they have no known competing financial interests or personal relationships that could have appeared to influence the work reported in this paper.

DATA AVAILABILITY

The data that support the findings of this study are available from the corresponding author, [DA], upon reasonable request.

REFERENCES

[1]   X. Zhang and J. W. Fergus, "Solid Electrolytes for Lithium Batteries," *International Journal of Technology*, vol. 9, no. 6, p. 1178, Dec. 2018, doi: 10.14716/ijtech.v9i6.2502.
[2]   X. Han *et al.*, "A comparative study of charging voltage curve analysis and state of health estimation of lithium-ion batteries in electric vehicle," *Automotive Innovation*, vol. 2, no. 4, pp. 263–275, Dec. 2019, doi: 10.1007/s42154-019-00080-2.
[3]   A. Rahali, K. E. Khadiri, and A. Tahiri, "Li-ion battery charger interface circuit with fast and safe charging for portable electronic devices," *Iranian Journal of Electrical and Electronic Engineering*, vol. 19, no. 1, 2023, doi: 10.22068/IJEEE.19.1.2527.
[4]   D. Anggraeni, B. Sudiarto, F. Kurniawan, and P. S. Priambodo, "Lithium-ion battery modelling and adaptive extended kalman filter implementation for BMS application Software Development," *International Journal of Renewable Energy Research*, vol. 13, no. 1, pp. 418–427, 2023, doi: 10.20508/ijrer.v13i1.12882.g8693.
[5]   J. Wei and C. Chen, "State of charge and health estimation for lithium-ion batteries using recursive least squares," in *2020 5th International Conference on Advanced Robotics and Mechatronics (ICARM)*, IEEE, Dec. 2020, pp. 686–689, doi: 10.1109/ICARM49381.2020.9195346.
[6]   R. Hiremath, S. Hulakund, V. R. Torgal, A. Patil, H. R. Patil, and A. B. Raju, "State-of-charge estimation using extended kalman filter," in *2023 International Conference for Advancement in Technology (ICONAT)*, IEEE, Jan. 2023, pp. 1–6, doi: 10.1109/ICONAT57137.2023.10080761.
[7]   B. Xia, G. Zhang, H. Chen, Y. Li, Z. Yu, and Y. Chen, "Verification platform of SOC estimation algorithm for lithium-ion batteries of electric vehicles," *Energies*, vol. 15, no. 9, p. 3221, Apr. 2022, doi: 10.3390/en15093221.
[8]   H. Aung, K. Soon Low, and S. Ting Goh, "State-of-charge estimation of lithium-ion battery using square root spherical unscented Kalman Filter (Sqrt-UKFST) in nanosatellite," *IEEE Transactions on Power Electronics*, vol. 30, no. 9, pp. 4774–4783, Sep. 2015, doi: 10.1109/TPEL.2014.2361755.
[9]   S. Kou, X. Gong, Q. Zhu, and G. Wang, "Parameter identification of battery model based on forgetting factor recursive least square method," in *2018 IEEE 4th Information Technology and Mechatronics Engineering Conference (ITOEC)*, IEEE, Dec. 2018, pp. 1712–1715, doi: 10.1109/ITOEC.2018.8740487.

[10] R. M. Imran, Q. Li, and F. M. F. Flaih, "An enhanced lithium-ion battery model for estimating the state of charge and degraded capacity using an optimized extended Kalman filter," *IEEE Access*, vol. 8, pp. 208322–208336, 2020, doi: 10.1109/ACCESS.2020.3038477.

[11] R. Guo and W. Shen, "Lithium-ion battery state of charge and state of power estimation based on a partial-adaptive fractional-order model in electric vehicles," *IEEE Transactions on Industrial Electronics*, vol. 70, no. 10, pp. 10123–10133, Oct. 2023, doi: 10.1109/TIE.2022.3220881.

[12] H. Beelen, H. J. Bergveld, and M. C. F. Donkers, "Joint estimation of battery parameters and state of charge using an extended Kalman Filter: a single-parameter tuning approach," *IEEE Transactions on Control Systems Technology*, vol. 29, no. 3, pp. 1087–1101, May 2021, doi: 10.1109/TCST.2020.2992523.

[13] M. Hossain, M. E. Haque, S. Saha, M. . Arif, and A. Oo, "State of charge estimation of li-ion batteries based on adaptive extended Kalman Filter," in *2020 IEEE Power & Energy Society General Meeting (PESGM)*, IEEE, Aug. 2020, pp. 1–5, doi: 10.1109/PESGM41954.2020.9282150.

[14] X. Li, Z. Huang, J. Tian, and Y. Tian, "State-of-charge estimation tolerant of battery aging based on a physics-based model and an adaptive cubature Kalman filter," *Energy*, vol. 220, p. 119767, Apr. 2021, doi: 10.1016/j.energy.2021.119767.

[15] Y. Jin, C. Su, and S. Luo, "Improved algorithm based on AEKF for state of charge estimation of lithium-ion battery," *International Journal of Automotive Technology*, vol. 23, no. 4, pp. 1003–1011, Aug. 2022, doi: 10.1007/s12239-022-0087-x.

[16] S. Yang, C. Zhang, J. Jiang, W. Zhang, L. Zhang, and Y. Wang, "Review on state-of-health of lithium-ion batteries: Characterizations, estimations and applications," *Journal of Cleaner Production*, vol. 314, p. 128015, Sep. 2021, doi: 10.1016/j.jclepro.2021.128015.

[17] S. K. Pradhan and B. Chakraborty, "Battery management strategies: An essential review for battery state of health monitoring techniques," *Journal of Energy Storage*, vol. 51, p. 104427, Jul. 2022, doi: 10.1016/j.est.2022.104427.

[18] R. Morello, R. Di Rienzo, R. Roncella, R. Saletti, and F. Baronti, "Hardware-in-the-loop platform for assessing battery state estimators in electric vehicles," *IEEE Access*, vol. 6, pp. 68210–68220, 2018, doi: 10.1109/ACCESS.2018.2879785.

[19] D. Anggraeni, B. Sudiarto, E. Fitrianingsih, and P. S. Priambodo, "Tuning window size to improve the accuracy of battery state-of-charge estimations due to battery cycle addition," *World Electric Vehicle Journal*, vol. 14, no. 11, p. 307, Nov. 2023, doi: 10.3390/wevj14110307.

[20] M. Lelie *et al.*, "Battery management system hardware concepts: an overview," *Applied Sciences*, vol. 8, no. 4, p. 534, Mar. 2018, doi: 10.3390/app8040534.

[21] T. Girijaprasanna and C. Dhanamjayulu, "A review on different state of battery charge estimation techniques and management systems for EV applications," *Electronics*, vol. 11, no. 11, p. 1795, Jun. 2022, doi: 10.3390/electronics11111795.

[22] D. Anggraeni *et al.*, "SoC estimation lithium polymer battery based on equivalent circuit model and extended Kalman Filter," in *2022 5th Asia Conference on Energy and Electrical Engineering (ACEEE)*, IEEE, Jul. 2022, pp. 118–122, doi: 10.1109/ACEEE56193.2022.9851867.

[23] L. Mattia, G. Petrone, F. Pirozzi, and W. Zamboni, "A low-cost approach to on-board electrochemical impedance spectroscopy for a lithium-ion battery," *Journal of Energy Storage*, vol. 81, p. 110330, Mar. 2024, doi: 10.1016/j.est.2023.110330.

[24] J. Wu *et al.*, "Design of a portable electrochemical impedance spectroscopy measurement system based on AD5941 for lithium-ion batteries," *Journal of Energy Storage*, vol. 84, p. 110856, Apr. 2024, doi: 10.1016/j.est.2024.110856.

[25] G. Crocioni, D. Pau, J.-M. Delorme, and G. Gruosso, "Li-ion batteries parameter estimation with tiny neural networks embedded on intelligent IoT microcontrollers," *IEEE Access*, vol. 8, pp. 122135–122146, 2020, doi: 10.1109/ACCESS.2020.3007046.

[26] X. Tian, B. Jeppesen, T. Ikushima, F. Baronti, and R. Morello, "Accelerating state-of-charge estimation in fpga-based battery management systems," in *6th Hybrid and Electric Vehicles Conference (HEVC 2016)*, Institution of Engineering and Technology, 2016, pp. 4 (6 .)-4 (6 .), doi: 10.1049/cp.2016.0964.

[27] P. Dinesh, K. K. Teja, S. Singh, S. M.P., and M. S., "FPGA based SoC estimator and constant current charging/discharging controller for lead–acid battery," in *2018 15th IEEE India Council International Conference (INDICON)*, IEEE, Dec. 2018, pp. 1–6, doi: 10.1109/INDICON45594.2018.8987133.

[28] S. Hong, M. Kang, H. Park, J. Kim, and J. Baek, "Real-time state-of-charge estimation using an embedded board for li-ion batteries," *Electronics*, vol. 11, no. 13, p. 2010, Jun. 2022, doi: 10.3390/electronics11132010.

[29] L. He, X. Hu, G. Yin, X. Shao, J. Liu, and Q. Shi, "A voltage dynamics model of lithium-ion battery for state-of-charge estimation by proportional-integral observer," *Applied Energy*, vol. 351, p. 121793, Dec. 2023, doi: 10.1016/j.apenergy.2023.121793.

[30] N. Shi, Z. Chen, M. Niu, Z. He, Y. Wang, and J. Cui, "State-of-charge estimation for the lithium-ion battery based on adaptive extended Kalman filter using improved parameter identification," *Journal of Energy Storage*, vol. 45, p. 103518, Jan. 2022, doi: 10.1016/j.est.2021.103518.

[31] S. Jiang and Z. Song, "A review on the state of health estimation methods of lead-acid batteries," *Journal of Power Sources*, vol. 517, p. 230710, Jan. 2022, doi: 10.1016/j.jpowsour.2021.230710.

[32] L. Canals Casals, M. Rodríguez, C. Corchero, and R. E. Carrillo, "Evaluation of the end-of-life of electric vehicle batteries according to the state-of-health," *World Electric Vehicle Journal*, vol. 10, no. 4, p. 63, Oct. 2019, doi: 10.3390/wevj10040063.

[33] T. Volan, C. R. Vaz, and M. Uriona-Maldonado, "Scenarios for end-of-life (EOL) electric vehicle batteries in China," *Revista de Gestão*, vol. 28, no. 4, pp. 335–357, Dec. 2021, doi: 10.1108/REGE-12-2020-0143.

BIOGRAPHIES OF AUTHORS

Dewi Anggraeni has a bachelor's degree in Engineering Physics from Institut Teknologi Sepuluh Nopember Surabaya, Indonesia, and a master's degree in electrical engineering from the University of Indonesia. She had a doctoral degree from the University of Indonesia. She has been working as a researcher in the Centre for Satellite Technology, BRIN (formerly Indonesian National Institute of Aeronautics and Space, LAPAN), Indonesia. Her research focuses on battery management systems, measurement systems, and signal processing technology, which also includes the design, analysis, and development of satellite power systems. She can be contacted at email: dewi.anggraeni@brin.go.id.

Budi Sudiarto 🆔 📊 SC ⓒ finished his bachelor's, master's, and Dr.-Ing. of Electrical Engineering from University of Indonesia (UI) and University of Duisburg-Essen (UDE), Germany, in 2001, 2004, and 2017. His research is concerned with Electrical Engineering, especially on power quality, renewable energy, and smart grid. His dissertation, when finished a Dr. -Ing. at UDE, is about disturbances in the grid system caused by household appliances. He can be contacted at email: budi.sudiarto@ui.ac.id.

Eriko Nasemudin Nasser 🆔 📊 SC ⓒ has a Bachelor's Degree in Aeronautics and Astronautics Engineering, Bandung Institute of Technology, Indonesia, and a master's degree in Space Engineering from TU Berlin, Germany. He has been working as a researcher in the Centre for Satellite Technology, BRIN (formerly Indonesian National Institute of Aeronautics and Space, LAPAN), Indonesia. His research focuses on space mission design and satellite technology, which also includes the design, analysis, and development of satellite systems and subsystems. He can be contacted at email: erik001@brin.go.id.

Wahyudi Hasbi 🆔 📊 SC ⓒ is an aerospace scientist and engineer with significant achievements in satellite technology. Graduating from Hasanuddin University with a Physics degree, he furthered his education with an M.Sc. in Computer Science from IPB University and a Ph.D. in Engineering, specializing in satellite systems from Technische Universität Berlin, achieving Summa Cum Laude honors. He is the current Head of the Research Center for Satellite Technology at the National Research & Innovation Agency of Indonesia (BRIN), playing a key role in the development of Indonesia's first microsatellite, LAPAN-TUBSAT, and subsequent satellites, LAPAN-A2/ORARI and LAPAN-A3/IPB. A Senior Member of both IEEE and AIAA, he has been honored internationally, including being elected an academician of the International Academy of Astronautics in 2023. Dr. Hasbi has held significant positions such as IEEE Indonesia Section Chair and chairs the Indonesian Satellite Society, with a distinguished role in the Asia Pacific Telecommunity. His contributions to satellite design and development have been recognized nationally, including receiving the prestigious Satyalancana Wirakarya from the President of Indonesia. With over 50 publications, his research focuses on microsatellites, satellite systems, and communications. He can be contacted at email: wahyudi.hasbi@brin.go.id.

Yus Natali 🆔 📊 SC ⓒ received her B.Eng.(S.T.) degree in telecommunication engineering from Sekolah Tinggi Teknologi Telkom, Bandung, in 2001, and the M.Eng.(M.T.) degree in telecommunication engineering from the Department of Electrical Engineering, University of Indonesia, Depok, in 2009, where she graduated with a doctoral (Dr.) degree in electrical engineering in 2023. She has been a Lecturer at Akademi Telkom Sandhy Putra Jakarta since 2003, and the Telkom University in Jakarta, Indonesia, since 2023. She has been the Head of the Telecommunications Engineering Study Program, Akademi Telkom Sandhyputra Jakarta, from 2012 to 2016 and 2023 until now at Telkom University. Her research interests include radio over fiber, distributed antenna systems, microwave photonics, wireless communication, integrated antenna electro-optic modulator, and wireless optical technology. She is also one of the editors of JICT Telkom University. She can be contacted at email: yusnatali@telkomuniversity.ac.id.

Purnomo Sidi Priambodo 🆔 📊 SC ⓒ received the B.S. degree in electrical engineering from Universitas Gadjah Mada, Indonesia, in 1987, the M.S. degree from the School of Electrical and Computer Engineering, Oklahoma State University, Stillwater, in 1996, and the Ph.D. degree in photonics and diffractive optics from the Department of Electrical Engineering, University of Texas at Arlington, in 2003. From 1987 to 1994, he joined PT Indosat. His job work experience spans from satellite earth stations to data communication and system programs. From 2003 to 2005, he was a Postdoctoral Fellow and a Senior Research Scientist at Resonant Sensors Inc., UT Arlington, USA. He joined the Department of Electrical Engineering, University of Indonesia, in 2007, where he has held a position as an associate professor in optoelectronics engineering since 2017. He has a U.S. patent disclosure on nonlinear optical guided-mode resonance filters and has published several papers on guided-mode resonance filters and devices. He has been a reviewer for various professional journals. He has been a member of the IEEE Lasers and Electro-Optics Society (LEOS) since 1996. He is also a member of the Honour Societies of Eta Kappa Nu and Phi Beta Delta. His research interests include diffractive optics, optical interconnection, quantum optoelectronics, semiconductor lasers, finite-difference time-domain electromagnetic propagation analysis, modulators/receivers, optical waveguides, photonic crystals, quantum electrodynamics, free-space optical communications, and, lately, infrared tomography. In 2024, Dr. Priambodo was appointed a full professor in the biomedical optoelectronics field. He can be contacted at email: purnomo.sidhi@ui.ac.id.